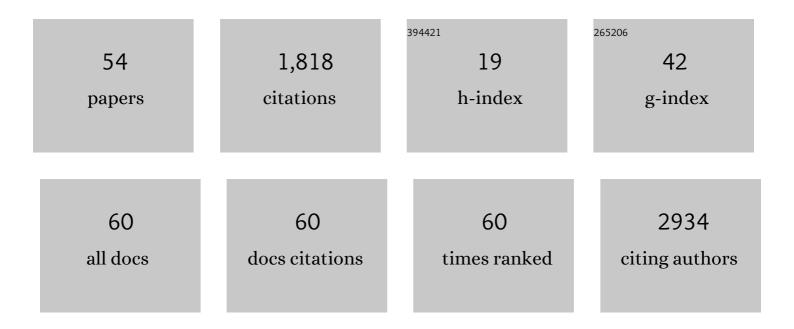
Jakub Jaroszewicz

List of Publications by Year in descending order

Source: https://exaly.com/author-pdf/4807463/publications.pdf Version: 2024-02-01



LAKUB LADOSZEWICZ

#	Article	IF	CITATIONS
1	Microfluidic-enhanced 3D bioprinting of aligned myoblast-laden hydrogels leads to functionally organized myofibers inÂvitro and inÂvivo. Biomaterials, 2017, 131, 98-110.	11.4	252
2	3D bioprinting of BM-MSCs-loaded ECM biomimetic hydrogels for <i>in vitro</i> neocartilage formation. Biofabrication, 2016, 8, 035002.	7.1	211
3	Gelatin methacrylate scaffold for bone tissue engineering: The influence of polymer concentration. Journal of Biomedical Materials Research - Part A, 2018, 106, 201-209.	4.0	122
4	Characterization of a Degraded Cadmium Yellow (CdS) Pigment in an Oil Painting by Means of Synchrotron Radiation Based X-ray Techniques. Analytical Chemistry, 2009, 81, 2600-2610.	6.5	121
5	3D bioprinting of hydrogel constructs with cell and material gradients for the regeneration of full-thickness chondral defect using a microfluidic printing head. Biofabrication, 2019, 11, 044101.	7.1	120
6	3D bioprinted hydrogel model incorporating <i>β</i> -tricalcium phosphate for calcified cartilage tissue engineering. Biofabrication, 2019, 11, 035016.	7.1	82
7	Highly ordered and tunable polyHIPEs by using microfluidics. Journal of Materials Chemistry B, 2014, 2, 2290.	5.8	80
8	3Dâ€Printing of Functionally Graded Porous Materials Using Onâ€Demand Reconfigurable Microfluidics. Angewandte Chemie - International Edition, 2019, 58, 7620-7625.	13.8	73
9	Correlation between porous texture and cell seeding efficiency of gas foaming and microfluidic foaming scaffolds. Materials Science and Engineering C, 2016, 62, 668-677.	7.3	70
10	Synthesis of porous hierarchical geopolymer monoliths byÂice-templating. Microporous and Mesoporous Materials, 2015, 215, 206-214.	4.4	65
11	Microfluidic Foaming: A Powerful Tool for Tailoring the Morphological and Permeability Properties of Sponge-like Biopolymeric Scaffolds. ACS Applied Materials & Interfaces, 2015, 7, 23660-23671.	8.0	55
12	Three-dimensional printed polycaprolactone-based scaffolds provide an advantageous environment for osteogenic differentiation of human adipose-derived stem cells . Journal of Tissue Engineering and Regenerative Medicine, 2018, 12, e473-e485.	2.7	46
13	In vitro degradation of ZM21 magnesium alloy in simulated body fluids. Materials Science and Engineering C, 2016, 65, 59-69.	7.3	39
14	Surface Modification of 3D Printed Polycaprolactone Constructs via a Solvent Treatment: Impact on Physical and Osteogenic Properties. ACS Biomaterials Science and Engineering, 2019, 5, 318-328.	5.2	38
15	Micro CT-based multiscale elasticity of double-porous (pre-cracked) hydroxyapatite granules for regenerative medicine. Journal of Biomechanics, 2012, 45, 1068-1075.	2.1	32
16	Electric Field Assisted Microfluidic Platform for Generation of Tailorable Porous Microbeads as Cell Carriers for Tissue Engineering. Advanced Functional Materials, 2018, 28, 1800874.	14.9	32
17	Preparation of a TiB2 composite with a nickel matrix by pulse plasma sintering with combustion synthesis. Journal of the European Ceramic Society, 2006, 26, 2427-2430.	5.7	31
18	Chitosan and composite microsphere-based scaffold for bone tissue engineering: evaluation of tricalcium phosphate content influence on physical and biological properties. Journal of Materials Science: Materials in Medicine, 2015, 26, 143.	3.6	30

JAKUB JAROSZEWICZ

#	Article	IF	CITATIONS
19	Insights into the macroporosity of freeze-cast hierarchical geopolymers. RSC Advances, 2016, 6, 24635-24644.	3.6	27
20	Formation of calcium phosphate coatings within polycaprolactone scaffolds by simple, alkaline phosphatase based method. Materials Science and Engineering C, 2019, 96, 319-328.	7.3	21
21	Novel optical photothermal infrared (O-PTIR) spectroscopy for the noninvasive characterization of heritage glass-metal objects. Science Advances, 2022, 8, eabl6769.	10.3	18
22	Naturally Formed Chitinous Skeleton Isolated from the Marine Demosponge Aplysina fistularis as a 3D Scaffold for Tissue Engineering. Materials, 2021, 14, 2992.	2.9	17
23	Possibilities and limitations of synchrotron X-ray powder diffraction with double crystal and double multilayer monochromators for microscopic speciation studies. Spectrochimica Acta, Part B: Atomic Spectroscopy, 2009, 64, 775-781.	2.9	16
24	The rheological and mechanical properties of magnetic hybrid membranes for gas mixtures separation. Materials Letters, 2016, 183, 170-174.	2.6	14
25	Micro and nanoscale characterization of poly(DL-lactic-co-glycolic acid) films subjected to the L929 cells and the cyclic mechanical load. Micron, 2018, 115, 64-72.	2.2	12
26	Engineering Human-Scale Artificial Bone Grafts for Treating Critical-Size Bone Defects. ACS Applied Bio Materials, 2019, 2, 5077-5092.	4.6	12
27	Functionalization of 3D Chitinous Skeletal Scaffolds of Sponge Origin Using Silver Nanoparticles and Their Antibacterial Properties. Marine Drugs, 2020, 18, 304.	4.6	12
28	Nanocrystalline Cu-Al ₂ 0 ₃ Composites Sintered by the Pulse Plasma Technique. Solid State Phenomena, 2006, 114, 227-232.	0.3	11
29	Insight into characteristic features of cartilage growth plate as a physiological template for bone formation. Journal of Biomedical Materials Research - Part A, 2016, 104, 357-366.	4.0	11
30	Investigation of mechanical properties of porous composite scaffolds with tailorable degradation kinetics after <i>in vitro</i> degradation using digital image correlation. Polymer Composites, 2017, 38, 2402-2410.	4.6	11
31	Pulse Plasma Sintering of Nano-Crystalline Cu Powder. Solid State Phenomena, 2006, 114, 239-244.	0.3	10
32	Osteogenesis around CaPâ€coated titanium implants visualized using 3D histology and microâ€computed tomography. Journal of Biomedical Materials Research - Part A, 2015, 103, 3463-3473.	4.0	10
33	A comparison of the microstructure-dependent corrosion of dual-structured Mg-Li alloys fabricated by powder consolidation methods: Laser powder bed fusion vs pulse plasma sintering. Journal of Magnesium and Alloys, 2022, 10, 3553-3564.	11.9	10
34	Characterization of Single-Crystal Dendrite Structure and Porosity in Nickel-Based Superalloys Using X-Ray Micro-Computed Tomography. Advanced Materials Research, 0, 278, 66-71.	0.3	9
35	Characterization of Three-Dimensional Printed Composite Scaffolds Prepared with Different Fabrication Methods. Archives of Metallurgy and Materials, 2016, 61, 645-650.	0.6	9
36	Skeletal ontogeny in basal scleractinian micrabaciid corals. Journal of Morphology, 2013, 274, 243-257.	1.2	8

0

#	Article	IF	CITATIONS
37	Thermal properties of multilayer graphene and hBN reinforced copper matrix composites. Journal of Thermal Analysis and Calorimetry, 2019, 138, 3873-3883.	3.6	8
38	X-ray physics-based CT-to-composition conversion applied to a tissue engineering scaffold, enabling multiscale simulation of its elastic behavior. Materials Science and Engineering C, 2019, 95, 389-396.	7.3	8
39	Analysis of Microstructure and Properties of a Ti–AlN Composite Produced by Selective Laser Melting. Materials, 2020, 13, 2218.	2.9	8
40	Scaffold vascularization method using an adipose-derived stem cell (ASC)-seeded scaffold prefabricated with a flow-through pedicle. Stem Cell Research and Therapy, 2020, 11, 34.	5.5	8
41	Advantages of combined μ-XRF and μ-XRD for phase characterization of Ti–B–C ceramics compared with conventional X-ray diffraction. Analytical and Bioanalytical Chemistry, 2008, 391, 1129-1133.	3.7	7
42	Fracture safety of double-porous hydroxyapatite biomaterials. Bioinspired, Biomimetic and Nanobiomaterials, 2016, 5, 24-36.	0.9	7
43	3Dâ€Printing of Functionally Graded Porous Materials Using Onâ€Đemand Reconfigurable Microfluidics. Angewandte Chemie, 2019, 131, 7702-7707.	2.0	6
44	Micro-analytical characterization of thorium-rich aggregates from Norwegian NORM sites (Fen) Tj ETQq0 0 0 rgB1	/Oyerlock	2 10 Tf 50 46
45	Energy Harvesting: Electric Field Assisted Microfluidic Platform for Generation of Tailorable Porous Microbeads as Cell Carriers for Tissue Engineering (Adv. Funct. Mater. 20/2018). Advanced Functional Materials, 2018, 28, 1870133.	14.9	4
46	Structural Aspects and Characterization of Structure in the Processing of Titanium Grade4 Different Chips. Metals, 2021, 11, 101.	2.3	4
47	Discussion: Fracture safety of double-porous hydroxyapatite biomaterials. Bioinspired, Biomimetic and Nanobiomaterials, 2016, 5, 176-177.	0.9	3
48	Corrosion Resistance of Aluminum Coatings Deposited by Warm Spraying on AZ91E Magnesium Alloy. Corrosion, 2019, 75, 668-679.	1.1	3
49	From Matrix Vesicles to Miniature Rocks: Evolution of Calcium Deposits in Calf Costochondral Junctions. Cartilage, 2021, 13, 326S-335S.	2.7	3
50	Ultrashort Sintering and Near Net Shaping of Zr-Based AMZ4 Bulk Metallic Glass. Materials, 2021, 14, 5862.	2.9	3
51	High-resolution microscopy assisted mechanical modeling of ultrafine electrospun network. Polymer, 2021, 230, 124050.	3.8	1
52	Modified Histopathological Protocol for Poly-É›-Caprolactone Scaffolds Preserving Their Trabecular, Honeycomb-like Structure. Materials, 2022, 15, 1732.	2.9	1

53	Nanocrystalline Cemented Carbides Sintered by the Pulse Plasma Method. Solid State Phenomena, 2006, 114, 245-250.	0.3	0	

54 From Micro-CT to Multiscale Mechanics of Double-Porous Hydroxyapatite Granules for Regenerative Medicine. , 2012, , .